ISSN 1070-3632, Russian Journal of General Chemistry, 2014, Vol. 84, No. 1, pp. 108–114. © Pleiades Publishing, Ltd., 2014.
Original Russian Text © O.R. Simonova, S.V. Zaitsev, O.I. Koifman, 2014, published in Zhurnal Obshchei Khimii, 2014, Vol. 84, No. 1, pp. 114–120.

Effect of Metal Cation Surrounding on the Redox Properties of Aluminum Porphyrinate in the Reaction with Organic Peroxide

O. R. Simonova[a], S. V. Zaitsev[a], and O. I. Koifman[a,b]

[a] *Krestov Institute of Solution Chemistry, Russian Academy of Sciences, ul. Akademicheskaya 1, Ivanovo, 153045 Russia*
e-mail: svz@isc-ras.ru

[b] *Ivanovo State University of Chemical Technology, Ivanovo, Russia*

Received February 21, 2013

Abstract—Intermolecular interaction of aluminum(III) 5,15-di(*o*-methoxyphenyl)-2,8,12,18-tetrabutyl-3,7,13.17-tetramethylporphyrinate chloride with bis(1-methyl-1-phenylethyl)peroxide has been studied by spectral and modeling methods; the reaction kinetics and mechanism have been elucidated. Effect of nature of the metal outer coordination sphere on the reaction rate has been examined. Geometry parameters of the initial molecules and the intermediates have been simulaed by the PM3 method, and their distortion has been estimated. The intermediates formation is accompanied by increased steric strain of the macrocycle.

DOI: 10.1134/S1070363214010174

Metal porphyrinates are known for variety of structural features reflected in their peculiar properties and thus numerous applications in modeling the biological systems as well as developing the active components of catalysts in technology [1–6]. The approaches to control the utilitarian properties of porphyrins and elucidation of their reactions mechanisms have remained topical issues in the field of macrocycles chemistry.

In view of that, this paper extended the previously reported studies of structure and properties of macrocyclic complexes of aluminum [7–10]. In particular, we studied the influence of the surrounding of the coordination site of aluminum(III) 5,15-di(*o*-mthoxyphenyl)-2,8,12,18-tetrabutyl-3,7,13.17-tetramethylporphyrinate chloride [(Cl)AlP] on its reactivity towards interaction with bis(1-methyl-1-phenylethyl)-peroxide (dicumyl peroxide). The reaction was studied by spectrophotometry [11] and by computer simulation [12–14].

Theoretical modeling was performed with the PM3 quantum-chemical method. The computed geometry and energy parameters are collected in Table 1. The (Cl)AlR molecule was nonplanar, of the C_{4v} symmetry (Fig. 1). Deformations of the *dome* and *saddle* types were operating in determining the spacial structure. The interaction of aluminum porphyrinate with peroxide led to formation of the intermediates containing the highly distorted macrocycles (Fig. 2). Besides the above-mentioned deformation types, *grooving* was observed (Fig. 1). Such conformation transformations significantly changed the molecule geometry, and therefore distorted the conjugation of π-electron system or even destroyed the chromophore structure.

With changing the metal cation surrounding by introducing imidazole molecule to the outer coordination sphere, the macrocycle symmetry was retained, however, the quantitative parameters of the molecule deformation were altered. The modeling revealed that the two structural types of the isolated complex molecules were the most probable: the base could be oriented at the side of the acido ligand [(Cl)(Im)AlP] or in the *trans*-position relative to chlorine [(Cl)Al(Im)P]. In the course of reaction with dicumyl peroxide, those compounds underwent strong two-dimensional and torsion deformations (Figs. 1, 2, Table 1) The structure of the intermediate was extremely unstable and the probability of its destruction was fairly high.

The absence of changes in electron absorption spectra typical of coordination processes revealed that

Table 1. Selected geometry parameters of (Cl)AlP and the reaction intermediates[a]

Complex	Al–N^{22} Al–N^{24}, Å	Al–N^{21} Al–N^{23}, Å	N^{21}–N^{23} N^{22}–N^{24}, Å	C_m–OR C_α–OR, Å	Al–Cl, Å	Ct–Al, Å	Al–N_L, Å	P_{N4}[b], Å	$N^{21}AlN^{24}$ $C^{19}N^{24}Al$, deg	$C^1C^{20}C^{19}$ $C^9C^{10}C^{11}$, deg	$C^{20}C^{19}C^{18}$ $C^2C^1C^{20}$, deg	$C^{20}C^{19}N^{24}$ $C^{18}C^{19}N^{24}$, deg
(Cl)AlP	2.431	1.821	4.117		2.306	0.507		11.667	78.121	127.702	121.523	129.147
	1.837	2.422	4.143						129.154	127.467	124.388	110.482
(Cl)AlP(OR)$_\alpha$(OR)$_m$	2.412	1.801	4.037	1.422	2.307	0.615		11.487	74.214	118.957	108.475	115.034
	1.781	2.423	4.069	1.407					134.941	127.341	122.022	101.658
(Cl)(Im)AlP[c]	2.539	1.623	4.082		2.456	0.707	1.915	11.519	82.214	124.957	123.876	125.754
	1.862	2.528	4.056						114.290	123.451	124.472	110.083
(Cl)(Im)AlP(OR)$_\alpha$(OR)$_m$	1.881	1.858	3.886	1.557	2.452	1.029	1.908	11.263	78.258	116.576	107.770	112.472
	2.418	2.556	4.019	1.544					123.270	123.348	124.486	102.542
(Cl)Al(Im)P[d]	1.821	2.420	4.157		2.345	0.449	2.445	11.790	79.410	128.386	121.942	128.102
	2.409	1.835	4.190						128.771	127.661	124.887	109.973
(Cl)Al(Im)P(OR)$_\alpha$(OR)$_m$	1.834	2.431	4.236	1.434	2.413	0.543	1.945	11.867	77.411	118.365	112.172	117.827
	2.468	1.809	4.159	1.426					133.29	127.312	122.931	102.055

[a] The atoms in the macrocycle are numbered according to the IUPAC nomenclature. [b] P_{N4} is perimeter of the coordination plane N_4. [c] *cis*-Position with respect to the imidazole acido ligands. [d] *trans*-Position with respect to the imidazole acido ligands.

the interaction of aluminum porphyrinates with dicumyl peroxide in *o*-xylene occurred at the peripheral part of the macrocycle to form the bond of the aryloxy groups with *meso*- and α-carbons (C_α–OR and C_m–OR) (Scheme 1) [15–19]. The intermediate was a sterically strained and therefore unstable compound that further degraded into the colorless products (Fig. 3a).

The reaction of aluminum porphyrinate [$c_{(Cl)AlR}$ = 3.2×10^{-6}–1.3×10^{-5} mol/L) with dicumyl peroxide ($c_{peroxide}$ = 2.3×10^{-7} mol/L) proceeded upon strong illumination at T = 295 K.

The reaction was of the pseudo-first order (n = 1) with respect to the peroxide, as followed from the

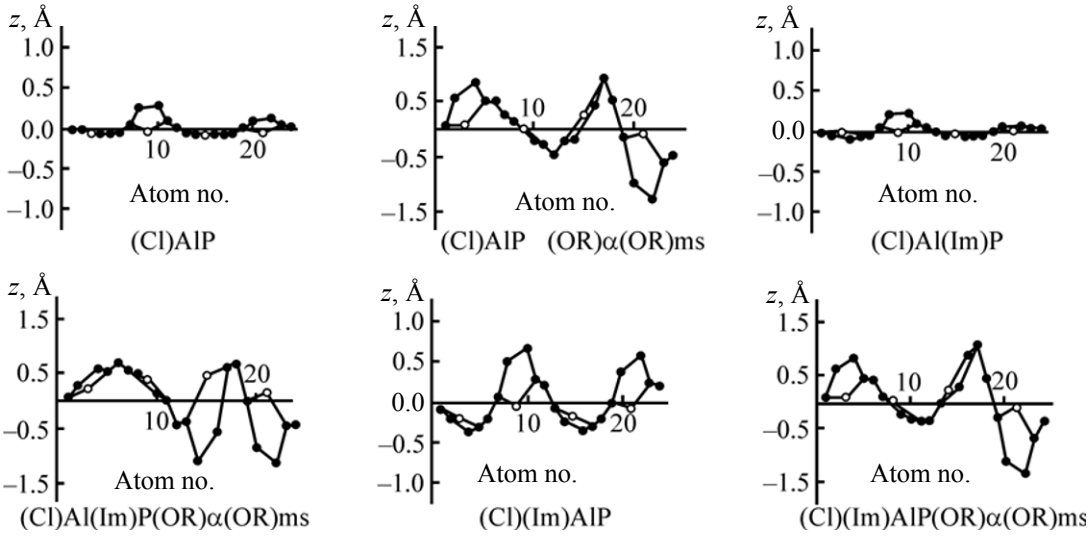

Fig. 1. Deviation of the tetrapyrrole macrocycle skeletal atoms from the mean plane along the z axis in (Cl)AlP and the intermediates of the reaction without (a) and in the presence of imidazole (b) (PM3 simulation); (○) nitrogen atoms, (●) carbon atoms.

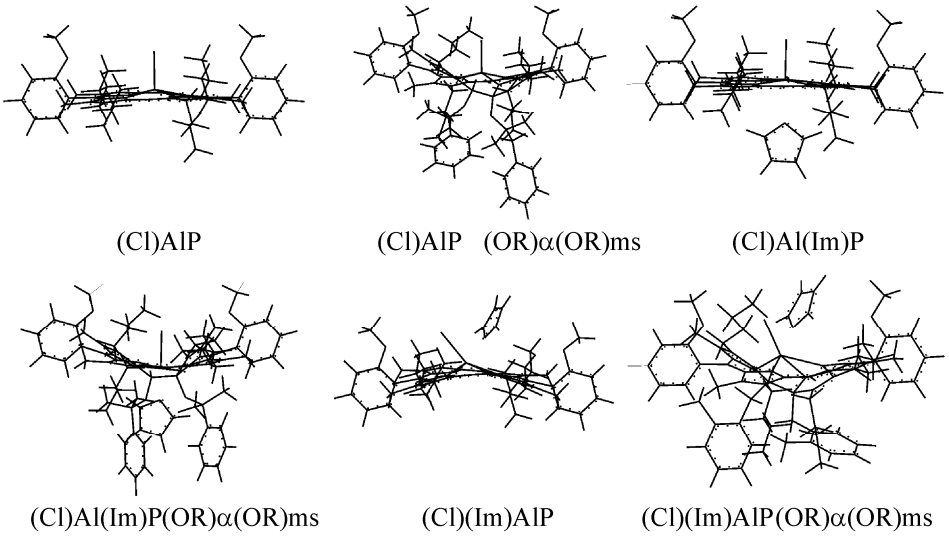

Fig. 2. Optimized structures of (Cl)AlP, (Cl)(Im)AlP, (Cl)Al(Im)P, and intermediates of the oxidation reaction (PM3 simulation).

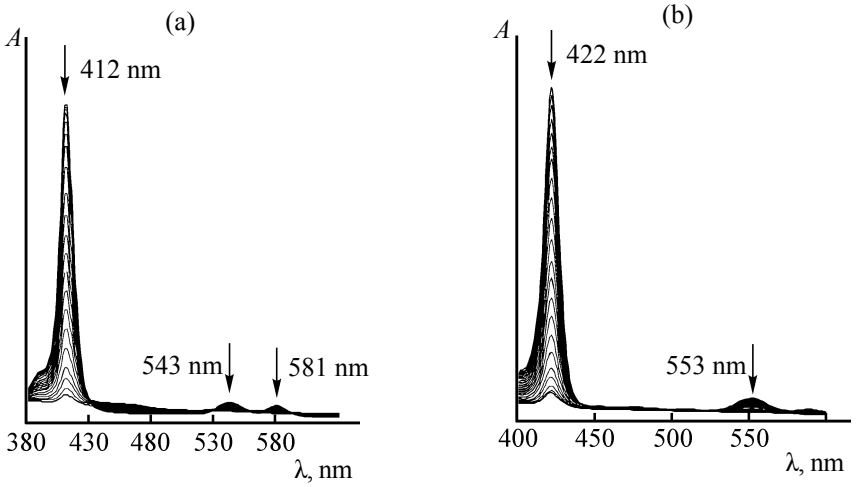

Fig. 3. Electron absorption spectra of (Cl)AlP in course of reaction with dicumyl peroxide ($c_{peroxide} = 0.23\times10^{-6}$ mol/L), $c_{(Cl)AlP} = 7.9\times10^{-6}$ mol/L, $c_{Im} = 0$ (a); $c_{(Cl)AlP} = 7.7\times10^{-6}$ mol/L, $c_{Im} = 4.5\times10^{-3}$ mol/L (b).

Scheme 1.

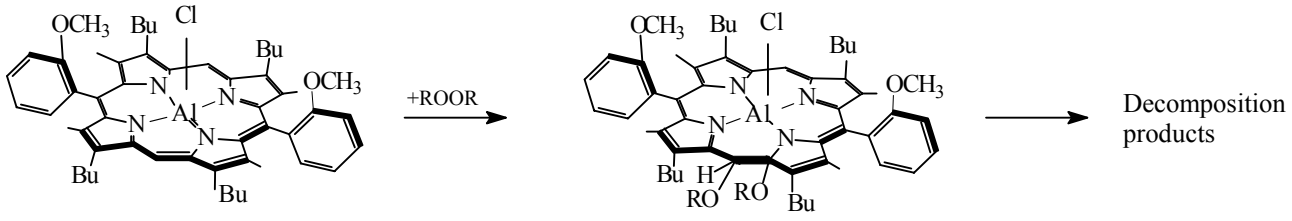

linear plot of $\ln(c_0/c_\tau) = f(t)$ and the nearly constant k_{eff} values (Fig. 4, Table 2).

$$-dc_{peroxide}/d\tau = kc^n_{peroxide}. \quad (1)$$

The effective rate constant k_{eff} was increasing linearly with the complex concentration. The reaction order with respect to the metal porphyrinate ($m = 1$) and the value of the true rate constant k_v (Fig. 5) were determined by fitting with the Eq. (2):

$$\log k_{eff} = \log k_v + m\log[(Cl)AlP]. \quad (2)$$

Hence, the rate equation of oxidation was as follows:

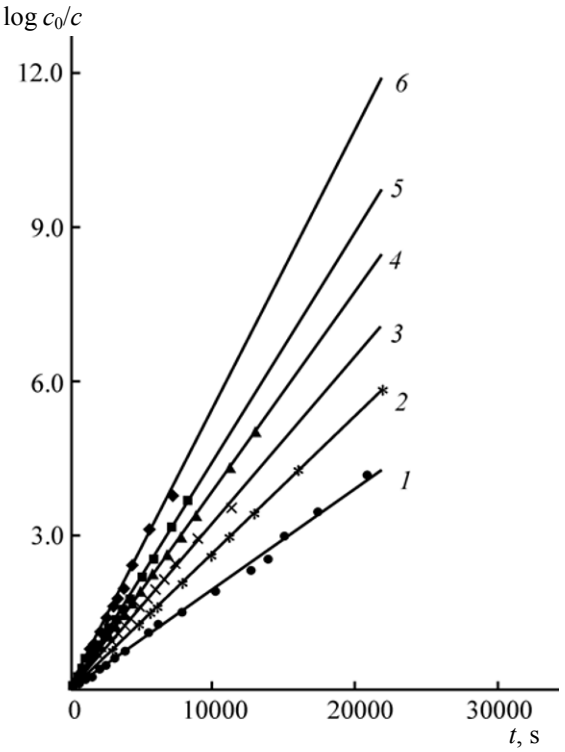

Fig. 4. Kinetic curves in the first order kinetics coordinates ($c_{peroxide}$ = 0.23×10^{-6} mol/L) at 295K, without imidazole: $c_{(Cl)AlP}$ = 3.20×10^{-6} mol/L (*1*), 4.50×10^{-6} mol/L (*2*), 6.8×10^{-6} mol/L (*3*), 7.90×10^{-6} mol/L (*4*), 9.90×10^{-6} mol/L (*5*), 1.33×10^{-5} mol/L (*6*).

$$-dc_{(Cl)AlP}/dt = k_v[(Cl)AlP]c_{peroxode} \quad (3)$$

In the presence of imidazole, the reaction proceeded via the above-described mechanism and was accompanied by destruction of the chromophore (Fig. 3b). However, introduction of the base into the macrocycle inner sphere led to changes in the reactant composition with the varied imidazole concentration [18], thus affecting the process rate. The molecular complex (Cl)Al(Im)P was the reactant in the presence of the base [7]. Formation of that complex was accompanied by the bands shift in the electron absorption spectrum (Fig. 6a) as well as by the shift of the macrocycle *meso*-protons and imidazole protons signals in the ^{1}H NMR spectrum (see Experimental). Using the restricted logarithmic method, we determined that aluminum porphyrinate and imidazole molecule reacted in the 1 : 1 ratio (Fig. 6b). The equilibrium constant K was of (1.39±0.07)×10^4 L/mol (Scheme 2).

The presence of imidazole (c_{Im} = 10^{-6}–10^{-4} mol/L) in the solution led to increase of k_v. At $c_{(Cl)AlR}$ = 3.2×10^{-6}–1.3×10^{-5} mol/L and $c_{peroxide}$ = 2.3×10^{-7} mol/L the reaction (Scheme 2) was of the first order with respect to the peroxide (n = 1) (Fig. 7, Table 2).

Scheme 2.

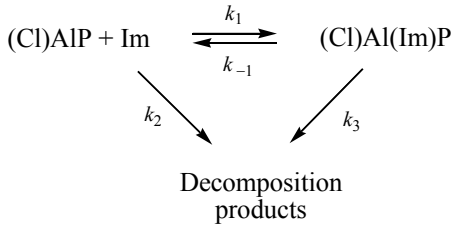

Noteworthily, the increase of the base concentration was accompanied by changes in the (Cl)AlP : (Cl)Al(Im)P ratio, the equilibrium was shifted towards the latter.

Table 2. Kinetic parameters of the reaction of (Cl)AlP with dicumyl peroxide at 295 K

$c_{(Cl)AlP}$×10^6, mol/L	k_{eff}×10^4, s^{-1}	$c_{(Cl)AlP}$×10^6, mol/L	k_{eff}×10^4, s^{-1}
$c_{peroxide}$ = 0.23×10^{-6} mol/L			
c_{Im} = 0 mol/L		c_{Im} = 4.5×10^{-6} mol/L	
3.2	1.98	2.1	1.66
4.5	2.66	3.5	2.19
6.8	3.33	5.1	2.97
7.9	3.96	7.1	3.78
9.9	4.62	9.9	4.92
13.3	5.38	11.2	5.41
k_v = 1.527 s^{-1} mol^{-1} L		k_v = 1.897 s^{-1} mol^{-1} L	
c_{Im} = 4.5×10^{-5} mol/L		c_{Im} = 4.5×10^{-4} mol/L	
3.1	2.54	2.7	2.47
4.1	2.98	4.0	3.11
6.1	4.10	4.8	3.59
7.5	4.90	5.7	4.27
		6.8	4.76
		7.7	5.78
k_v = 3.413 s^{-1} mol^{-1} L		k_v = 6.102 s^{-1} mol^{-1} L	
c_{Im} = 0.5×10^{-3} mol/L			
2.1	2.32	5.8	5.56
2.9	3.14	7.0	5.92
3.2	3.42	9.0	7.00
4.8	4.21		
k_v = 4.493 s^{-1} mol^{-1} L			

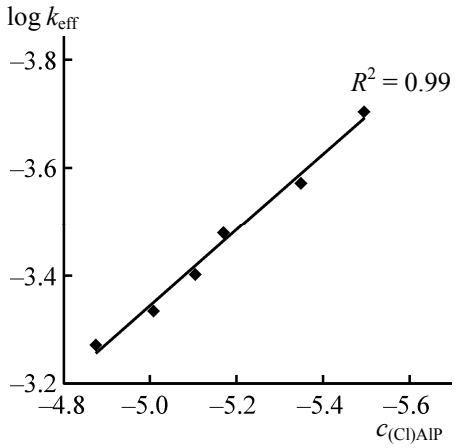

Fig. 5. Effective rate constant as function of concentration of aluminum porphyrinate ($c_{Im} = 0$).

The k_{eff} value was linear with the complex concentration, and the reaction order with respect to metal porphyrinate was of $m = 1$; the true rate constant was determined (Fig. 8, Table 2).

The rate equation of that reaction was as follows Eq. (4).

$$dc_A/dt = k_2[(Cl)AlP]c_{peroxide} + k_3[(Cl)Al(Im)P]c_{peroxide}, \quad (4)$$

$$[(Cl)Al(Im)P] = K_{eq}[(Cl)AlP][Im]. \quad (5)$$

with $K_{eq} = k_1/k_{-1}$ being the equilibrium constant. Substituting Eq. (5) into Eq. (4) one gets Eq. (6):

$$dc_A/dt = k_2[(Cl)AlP]c_{peroxide} + k_3K_{eq}[(Cl)AlP][Im]c_{peroxide} = [(Cl)AlP]c_{peroxide}(k_2 + k_3K_{eq}[Im]), \quad (6)$$

and then $k_3K_{eq}[Im] = k'_3$ gave Eq. (7).

$$k_3K_{eq}[Im] = k'_3,$$

$$dc_A/dt = (k_2 + k'_3)[(Cl)AlP]c_{peroxide}. \quad (7)$$

The overall constant $k_v = k_2 + k'_3$ characterizing the parallel reactions of both (Cl)AlP and (Cl)Al(Im)R was determined.

At imidazole concentration of 4.5×10^{-3} mol/L, the reagents were (Cl)Al(Im)P and dicumyl peroxide ($n = 1$, $m = 1$, Figs. 7 and 8). The rate equation was as follows:

$$dc_A/dt = k_v[(Cl)Al(Im)P]c_{peroxide}. \quad (8)$$

Further increase of k_v could be expected, as in the presence of (Cl)Al(Im)P the reaction was accelerated. However, the process rate started to decrease (Table 2), seemingly, due to deactivation of dicumyl peroxide with free imidazole (present in large excess) [20].

Calculated and experimental data were in good agreement; thus, computer simulation was proved to be a reasonable method to study the described interactions.

The nature of the metal cation surrounding as well as structural features of the periphery of the macrocycle significantly influenced the porphyrin ligand deformation. That led to partial loss of aromaticity and enhanced the basicity; as a consequence the kinetic

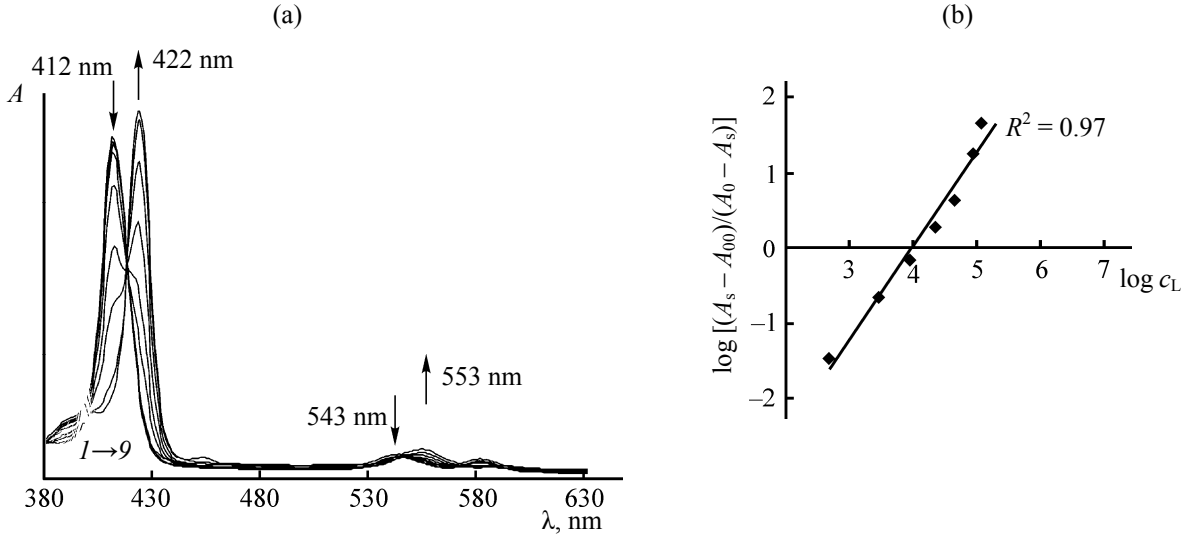

Fig. 6. Electron absorption spectra of (Cl)AlP in the course of reaction with imidazole (*1*) $c_{(Cl)AlP} = 8.03\times10^{-6}$ mol/L, $c_{Im} = 0$; (*2–8*) at intermediate concentrations of imidazole, $c_{Im} = 8.10\times10^{-6}$–$2.07\times10^{-3}$ mol/L, (*9*) in the excess of imidazole, $c_{Im} = 4.50\times10^{-3}$ mol/L, in *o*-xylene (a). Determination of the interaction stoichiometry (A_o, A_s, and A_∞: absorbance of metal porphyrinate, equilibrium mixtures, and the complex solutions at λ = 422 nm; tan α = 1) (b).

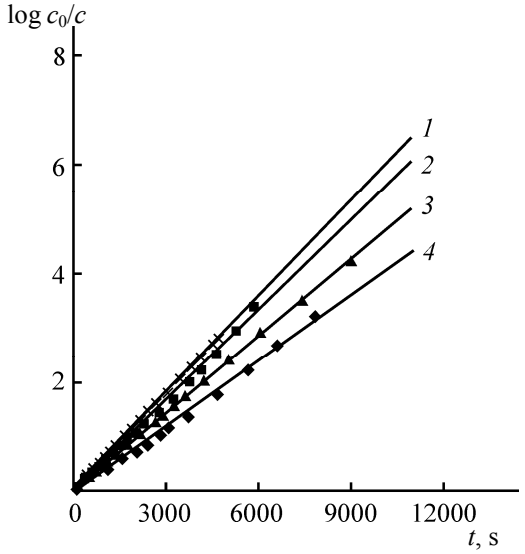

Fig. 7. Kinetic curves in the first order kinetics coordinates ($c_{peroxide}$ = 0.23×10^{-6} mol/L) at 295 K, c_{Im} = 4.5×10^{-6} mol/L (*1*), 4.5×10^{-5} mol/L (*2*), 4.5×10^{-4} mol/L (*3*), and 4.5×10^{-3} mol/L (*4*).

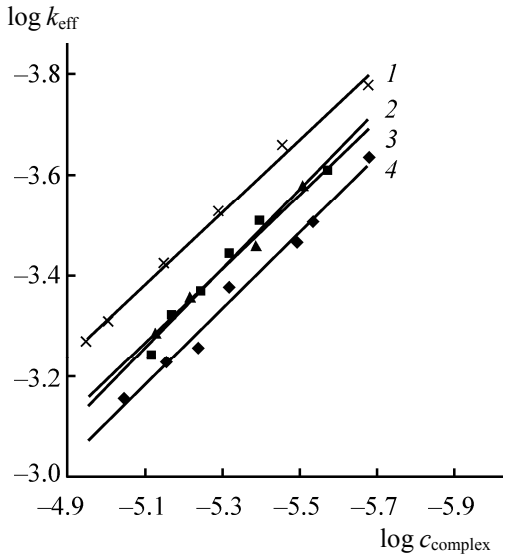

Fig. 8. Effective rate constant as function of the complex concentration in the presence of imidazole, c_{Im} = 4.5×10^{-6} mol/L (*1*), 4.5×10^{-5} mol/L (*2*), 4.5×10^{-4} mol/L (*3*), and 4.5×10^{-3} mol/L (*4*).

parameters were changed. The reaction rate was affected by the change in the reagent composition (due to altering concentration of the substrate introduced at the coordination site) as well.

EXPERIMENTAL

Electron absorption spectra were recorded with Cary 50 instrument at T = 295 K.

The reaction mixture was illuminated with medium pressure mercury lamp of TUNGSRAM type, 20W, F33.

The procedure of kinetic data processing was described in detail in [23]. The effective rate constant (k_{eff}) was determined from the changes in the optical density of the solution at (λ 412 or 422 nm) measured at regular time intervals. In the excess of aluminum porphyrinate, the formally first order Eq. (9) was used:

$$k_{eff} = 1/\tau \ln (c_0/c_\tau). \quad (9)$$

Here c_0, and c_τ are peroxide concentrations at time 0 and τ, respectively.

k_v and k_{eff} Values were determined by the least squares method with Microsoft Excel and ggh.exe (QB-45) software by the Guggenheim method. The relative error was 7–12%.

Quantum-chemical calculations were performed at the CNDO approximation level [24] via the PM3 method [12–14, 25] with full geometry optimization. The stopping condition was the gradient of 0.0004 kJ mol^{-1} Å^{-1}.

Aluminum(III) 5,15-di(*o*-methoxyphenyl)-2,8,12,18-tetrabutyl-3,7,13.17-tetramethylporphitinate chloride was prepared as described elsewhere [21, 22].

Porphyrin ligand. ^{1}H NMR spectrum ($CDCl_3$, external reference HMDS), δ, ppm: 10.20 s (2H, *ms*-H), 7.67d (2H, *o*-H, phenyl), 7.62 t (2H, *m*-H, phenyl), 7.21 t (2H, *p*-H, phenyl), 7.10 *d* (2H, *m*-H, phenyl), 3.98 t (8H, CH_2, butyl), 3.82 s (6H, OCH_3), 2.56 s (12H, CH_3), 2.18 m (8H, CH_2, butyl), 1.65 m (8H, CH_2, butyl group), 1.09 t (12H, CH_3, butyl), –2.36 s (2H, NH). Electron absorption spectrum in xylene, λ_{max}, nm (log ε): 412 (5.5) 543 (4.30) 581 (4.23).

(Cl)AlP. ^{1}H NMR spectrum ($CDCl_3$, external reference HMDS), δ, ppm: 9.95 s (2H, *ms*-H), 7.57 d (2H, *o*-H, phenyl), 7.14 m (6H, *m*,*p*-H, phenyl), 4.35 t (8H, CH_2, butyl), 4.12 s (6H, CH_3O), 2.54 s (12H, CH_3), 1.60 t (16H, CH_2CH_2, butyl), 1.03 t (12H, CH_3, butyl).

(Cl)Al(Im)P. ^{1}H NMR spectrum ($CDCl_3$, external reference HMDS), δ, ppm: 10.11 s (2H, *ms*-H), 7.68 s (3H, $H^{2,4,5}$), 7.10 s (1H, NH), 4.33 t (8H, CH_2, butyl), 4.10 s (6H, CH3O), 2.56 s (12H, CH_3), 1.70 m (16H, CH_2, butyl), 1.08 t (12H, CH_3, butyl).

Im. ^{1}H NMR spectrum ($CDCl_3$, external reference HMDS), δ, ppm: 8.47 s (1H, H^2), 7.75 s (2H, $H^{4,5}$), 7.15 s (H, NH).

ACKNOWLEDGMENTS

This work was financially supported by the program of the Russian Academy of Sciences "Theoretical and experimental study of the nature of chemical bonding and mechanisms of important chemical reactions and processes," no. 1, OHNM RAS 2011, and by the grants from the Russian Foundation for Basic Research (nos. 12-03-00824-a, 11-03-00993-a).

REFERENCES

1. Konovalova, N.V., Evstigneeva, R.P., and Luzgina, V.N., *Russ. Chem. Rev*., 2001, vol. 70, no. 11, p. 939.
2. Mamardashvili, G.M., Mamardashvili, N.Zh., and Koifman, O.I., *Russ. Chem. Rev*., 2005, vol. 74, no. 8, p. 765.
3. Mamardashvili, G.M., Mamardashvili, N.Zh., and Koifman, O.I., *Russ. Chem. Rev*., 2008, vol. 77, no. 1, p. 59.
4. Koifman, O.I. and Mamardashvilim, N.Zh., *Nanotechnol. in Russia*, 2009, vol. 4, nos. 5–6, p. 253.
5. Afanasiev, P., Bouchu, D., Kudrik, E.V., Millet, J.-M.M., and Sorokin, A.B., *Dalton Trans*., 2009, vol. 38, no. 44, p. 9828.
6. Kudrik, E.V., Afanasiev, P., Alvarez, L.X., and Dudourdeaux, P., *Nature Chem*., 2012, vol. 4, no. 12, p. 1024.
7. Zaitseva, S.V., Zdanovich, S.A., and Koifman, O.I., *Russ. J. Gen. Chem*., 2006, vol. 76, no. 10, p. 1660.
8. Sokolova, T.N., Lomova, T.N., Zaitseva, S.V., Zdanovich, S.A., Suslova, E.E., and Maizlish, V.E., *Russ. J. Inorg. Chem*., 2005, vol. 50, no. 3, p. 476.
9. Zaitseva, S.V., Zdanovich, S.A., and Koifman, O.I., *Russ. J. Coord. Chem*., 2010, vol. 36, no. 5, p. 323.
10. Sokolova, T.N., Lomova, T.N., Zaitseva, S.V., Zdanovich S.A., and Majzlish V.E., *Russ. J. Inorg. Chem*., 2008, vol. 53, no. 2, p. 220.
11. Bulatov, M.I. and Kalinkin, I.P., *Prakticheskoe rukovodstvo po fotokolometricheskim i spektrofotometricheskim metodam analiza* (Practical Guide to Photocolorimetry and Spectrophotometric Methods of Analysis), Leningrad: Khimiya, 1968.
12. Stewart, J.J.P., *J. Comput. Chem*., 1989, vol. 10, no. 2, p. 221.
13. Stewart, J.J.P., *J. Comp.-Aided Mol. Des*., 1990, vol. 4, p. 1.
14. Fletcher, R*., Methods of Optimization*, New York: John Wiley & Sons, 1980, p. 45.
15. Liston, D.J. and West, B.O., *Inorg. Chem*., 1985, vol. 24, no. 10, p. 1568.
16. Kalish, H., Camp, J.E., Stepien, M., Latos-Grazynski, L., and Balch, A.L., *J. Am. Chem. Soc*., 2001, vol. 123, no. 47, p. 11719.
17. Berezin, B.D. and Sennikova, G.V., *Kinetika i Kataliz*, 1968, vol. 9, no. 3, p. 528.
18. Simonova, O.R., Zaitseva, S.V., and Koifman, O.I., *Russ. J. Coord. Chem*., 2009, vol. 35, no. 5, p. 320.
19. Bagdasaryan, Kh.S., *Teoriya radikal'noi polimerizatsii* (Theory of Radical Polymerization), Moscow: Nauka, 1966, p. 300.
20. Cheremenskaya, O.V., Solov'eva, F.B., and Ponomarev, G.V., *Russ. J. Phys. Chem., A*, 2001, vol. 75, no. 10, p. 1633.
21. Lindsey, J.S. and Woodford, J.N., *Inorg. Chem*., 1995, no. 34, p. 1063.
22. Semeikin, A.S., Koifman, O.I., and Berezin, B.D., *Chem. Heterocyc. Comp.*, 1982, no. 10, p. 1046.
23. *Eksperimental'nye metody khimicheskoi kinetiki* (Experimental Methods of Chemical kinetics), Emanuel', N.M. and Sergeev, G.B., Eds., Moscow: Vysshaya Shkola, 1980.
24. Bersuker I.B., *Electronic Structure and Properties of Transition Metal Compounds*, New York: Willey, 1996.
25. Schidt, M.W., Baldridge, K.K., Boatz, J.A., Elbert, S.T., Gordon, M.S., Jensen, J.H., Koseki, S., Matsunaga, N., Nguyen, K.A., Su, S., Windus, T.L., Dupuis, M., and Montgomeri, J.A., *J. Comput. Chem*., 1993, vol. 14, no. 11, p. 1347.